Single-Phase Seven-Level Grid-Connected Photovoltaic System with Ripple Correlation Control Maximum Power Point Tracking

Sandeep. N*‡, Udaykumar R.Y**

*Research Scholar, Department of Electrical and Electronics Engineering, National Institute of Technology Karnataka (NITK), Surathkal, India, 575025

**Professor, Department of Electrical and Electronics Engineering, National Institute of Technology Karnataka (NITK), Surathkal, India, 575025

(sandeep.1991.in@ieee.org, udaykumar.yaragatti.in@ieee.org)

‡Corresponding Author; Sandeep. N, Department of Electrical & Electronics Engineering,

National Institute of Technology Karnataka (NITK), Surathkal, India -575025

Tel: +91 8951879158, sandeep.1991.in@ieee.org

Received: 04.06.2016 Accepted:06.08.2016

Abstract- This paper puts forward a control scheme for single-phase photovoltaic (PV) fed grid connected with cascade H-bridge (CHB) inverter. A unique control strategy based on the voltage ratio is proposed and is embedded with ripple correlation control (RCC) based maximum power point tracking (MPPT) to ensure the efficient energy conversion. The control scheme employed enables the independent operation and control of individual DC link voltage, ensuring the extraction of maximum power available from each PV panel. In addition, low harmonic grid currents are generated with an arbitrary power factor. Independent control of active and reactive power is exercised by decoupled component method. Numerical simulation was performed using the MATLAB/SIMULINK platform and results for three H-bridge cells connected in series are presented to support the theoretical concepts and control scheme proposed.

Keywords Maximum power point tracking, multilevel inverter, topology.

1. Introduction

The growing oil demand and depleting fossil fuel have led the use of power generated from renewable as an alternative. Since, the renewable energy generation is free from pollution, freely available, abundant in nature. Among the many sources available solar photovoltaics (PV) have gained a lot of interest. It has become a hotspot for researching and also people from academia have shown tremendous interest in coming up with new and highly efficient methods of power extraction. There has been exponential growth in the number of PV installations over the past decades, mainly, due to the support of government and participation of utilities in promoting green energy [1]. PV systems are mainly two types: standalone and grid connected. Grid connected PV has played a major role since most of the installation is of a grid interactive type. The technology of grid connected PV mainly includes a) string, b) centralized, c) multi-string, and d) AC module type [2]. In comparison to centralized, string architecture is capable of handling module mismatch and is more efficient thus has gained more commercial popularity. Multi-string structure involves a dedicated DC-DC converter for maximum power point tracking (MPPT) which is an essential and inevitable part of a high efficient PV system. However, the efficiency is not high due to cascading of DC-DC converter and inverter for processing power from PV to grid. Therefore, each approach has advantages and disadvantages; a tradeoff should be made between the harmonic generation, efficiency, complexity, reliability, safety, modularity and cost.

In the preceding years, multilevel inverters (MLI) have taken their way into PV applications [3]. The high quality waveform generation capability, low device switching frequency, and low EMI is the uncommon merits that have rendered them suitable for both high and low power PV applications [4]. Suitability and comparison of several types of multilevel inverter for grid connected applications is presented by the researchers [5]. It is worth noting that; though the number of power semiconductor devices is more in MLI; it comes with an advantage of the reduced filtering requirement, which implies less space, cost and increased efficiency. Among various MLI topologies available, significant ones are diode-clamped (DC) MLI, flying capacitor (FC) MLI, and cascade H-bridge (CHB) MLI. CHBMLI being the simplest among the three and also the requirement of isolated power sources for its operation has made it suitable and attractive for PV applications[6]. In addition to this it is also important to mention that it exhibits a higher degree of freedom of control and capability to operate under fault condition results in increased overall reliability of the system [7]. On the other hand CHBMLI suffers due to fact that the common mode voltage magnitude is high which calls for extra measures to suppress the ground leakage current. Many researchers have come up with a modified way of pulse width modulation (PWM) control, novel topologies, common mode inductor based filtering approach and many others to combat this issue which is out of scope of this paper [8-9].

For satisfactory and stable operation of a grid connected CHBMLI with *n* cells, independent control of the grid current and DC-link voltages are necessary [10-11]. This control can be carried out using the *n* modulating signals available, each for one modulating cell. In [12], the method proposed works only for equal DC link voltage which a not a practical solution for PV since it is greatly affected by the partial shading resulting in nonuniform DC link voltages. Passivity based controllers developed have been presented in [13] however, equations are not explicitly derived.

In this paper ripple correlation control (RCC) method based MPPT is applied to a single-phase seven level grid connected PV system. A simple voltage fraction based control system is developed and a proportional resonant controller is applied for grid current control. A simple voltage fraction based control system is developed and a proportional resonant (PR) controller is applied to grid side current control. Extensive simulation is performed using the MATLAB / SIMULINK platform in order to validate the control strategy developed. Simulation results demonstrating the superior performance and satisfactory operation of the proposed system for various operating conditions are presented.

2. Topology Description and the Proposed Control Method

Fig. 1. Shows the topology diagram of the proposed system consisting of three H-bridge cells connected in series to form a seven level CHBMLI each, fed by a string of PV panels/array. Each dc link is fed by a short string of PV panels. By considering cells with the same dc-link voltage, the converter can synthesize an output voltage v_{ab} with n levels. The output voltage can be expressed in terms of gating signals as $v_{ab} = (P_{1j} - P_{3j}) * v_{pvj},\ j = 1,...,n$. Where P_{XX} represents the state of each upper switch. If $P_{XX} = 1$ the corresponding switch is ON and if $P_{XX} = 0$ the corresponding switch is OFF.

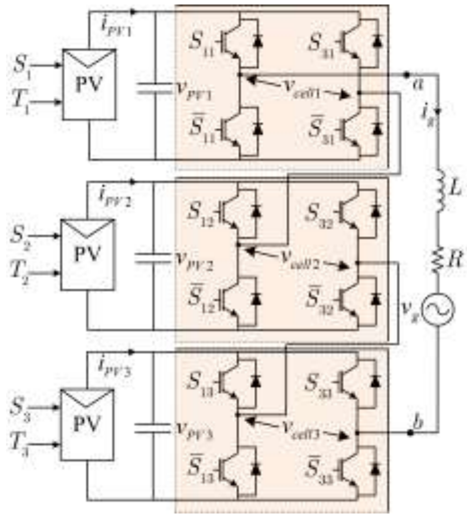

Fig. 1. Topology of the proposed single-phase seven level grid connected PV system

2.1. Principle of operation

All The CHBMLI are simply the interconnection of bridges capable of generating three level voltage outputs, *V, 0, -V*. The output AC voltage is the total of the three individual cell outputs resulting in the generation of seven levels stepped waveform. The high quality of the synthesized waveform at the output enables the reduction of harmonic components injecting a grid current with low total harmonic distortion. The relation between the number of output voltage levels and the cells is given by N_{level} = (2*H*+1), where, H is the number of cells connected in series. The method of pulse generation is outlined in the Fig. 2. A phase shifted PWM consisting of three identical high frequency triangular waveforms shifted by 60 degrees (Φ=360/(N_{level} -1)) and a grid frequency (f_g) reference sine wave is employed. The condition for pulse generation is as follows

$$S_{11} = \begin{cases} 1 & v_{ref} > v_{cr1} \\ 0 & v_{ref} < v_{cr1} \end{cases}$$

$$S_{12} = \begin{cases} 1 & v_{ref} > v_{cr2} \\ 0 & v_{ref} < v_{cr2} \end{cases}$$

$$S_{13} = \begin{cases} 1 & v_{ref} > v_{cr3} \\ 0 & v_{ref} < v_{cr3} \end{cases}$$

$$S_{31} = \begin{cases} 1 & v_{ref+180^0} > v_{cr1} \\ 0 & v_{ref+180^0} < v_{cr1} \end{cases}$$

$$S_{32} = \begin{cases} 1 & v_{ref+180^0} > v_{cr2} \\ 0 & v_{ref+180^0} < v_{cr2} \end{cases}$$

$$S_{33} = \begin{cases} 1 & v_{ref+180^0} > v_{cr3} \\ 0 & v_{ref+180^0} < v_{cr3} \end{cases}$$

The advantage of PSPWM is that the harmonic spectrum of output voltage with equal DC link voltage will have its first dominating harmonic of frequency equal to $2^*N_{level}\ ^*f_g$. From the normalized waveform shown in Fig. 2. It can be seen that the three-level voltage generated by each cell is summed up to form a seven level at the output.

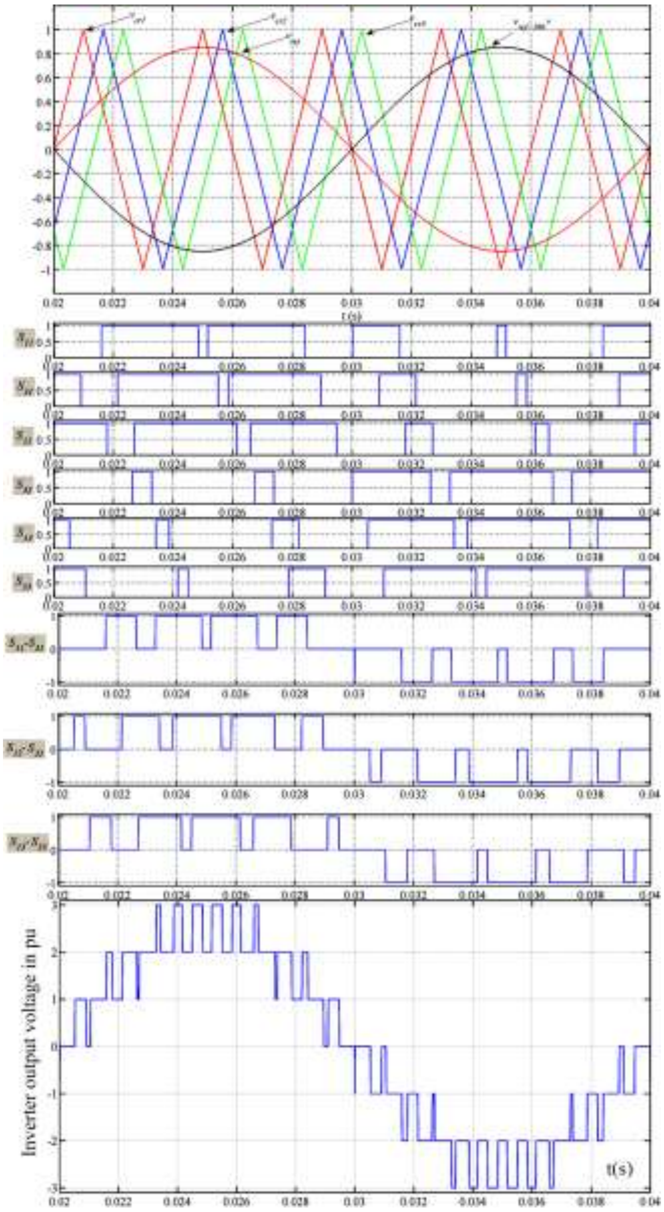

Fig. 2. Phase shifted PWM and switching pulse generation.

2.2. Proposed control scheme

The proposed control scheme for individual DC link voltage control is based on the classical control of grid connected MLI. The scheme is shown in Fig. 3. Which consist of *n+1* control loops; n loops are required for the control of DC link voltages and one loop for the control of sinusoidal grid current being injected. Each PV panel/array parameters (voltage and current) are sensed for ensuring the operating point near the maximum power point (MPP). The reference DC link voltage generated is compared with the actual sensed one and the error is processed through a PI

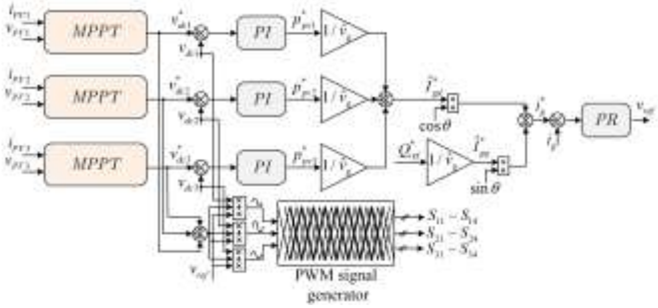

Fig. 3. Proposed control scheme.

controller. Depending upon the error the PI controller generates the power reference and if the power generated by PV is more than being drawn from it, then, the error is positive which increases the output of the PI controller and vice versa. The sum of the outputs of all the PI controller gives the total amount of power available from the PV and that needs to be dumped to the grid. The reference grid current is generated from this power using the relation $\hat{I}_{gd}^{*} = \dfrac{p_{pv1}^{*} + p_{pv2}^{*} + p_{pv3}^{*} + \ldots p_{pvn}^{*}}{\hat{v}_g}$. To control the active and reactive power injected into the grid, the reactive power control loop is embedded into the main loop as shown in Fig. 3. The proportional resonant controller generates the reference voltage corresponding to the error, in grid current and actual grid current reference. The modulation index for each cell is assigned being dependent on the ratio of each reference DC link to the sum of the (*n* DC link reference voltages). This enables and ensures the operation of each PV around the MPP corresponding to its own irradiation and temperature levels independent of each other.

2.3. RCC MPPT

Since the power generated by the PV depends upon the environmental condition mainly on the irradiation and its cell temperature level, it is important to keep the operating point around MPP for maximum energy conversion efficiency. MPPT is the method using which the operating point of the PV even with varying irradiation and temperature level can be made to vary around MPP. This is achieved by sensing the PV voltage and current and making the partial derivative of the change in PV power (δp) and voltage (δv) to zero. There are many techniques available for achieving this [14-17]. Among the several methods available RCC is found to be more suitable for single phase grid connected PV [18-21]. The high qulaity sinusoidal current injected into the grid results in sinusoidal power of twice the grid frequency as per the following equ. (1). Where V_{in} and i_{in} are input DC voltage and current. V_g and I_g corresponds to RMS grid voltage and grid current respectiveley. The charactersitics of PV is to supply double frequency i_{pv} and v_{pv} along with their DC components. Thus the DC link voltage and current will have inherent second harmonic components in them.

$$V_{in} i_{in} = V_g I_g \sin^2(\omega t) = \frac{V_g I_g}{2}(1-\cos(2\omega t)) \quad (1)$$

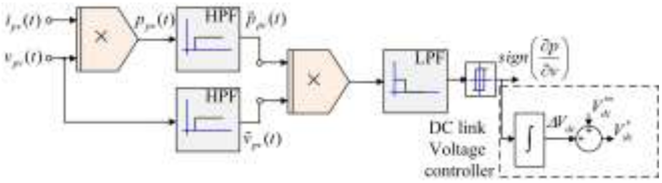

Fig. 4. RCC MPPT controller and DC link voltage regulator.

The crucks of RCC MPPT lies in the extraction of these voltage and/or current ripple due to switching action of the converter. The method find itself very suitable since the oscillation of power is inherent to single phase grid connected inverter system. The ouput voltage and power of PV panesl can be written as follows:

$$v(t) = \bar{v}(t) + \tilde{v}(t)$$
$$p(t) = \bar{p}(t) + \tilde{p}(t)$$

where $\bar{v}(t)$ and $\bar{p}(t)$ are the average value of PV voltage and power over a switching period. As long as the operating point is towards the left of MPP the oscillatory volatge ($\tilde{v}(t)$) and power ($\tilde{p}(t)$) components are in-phase with each other. As the operating traverses towards right from the MPP the oscillatary volatge and power components goes out-of phase with other. This information is used for keeping the operating point near MPP. These oscillatory components are extracted using high pass and low pass filters as shown in the block diagram of Fig. 4. Detailed information regarding the implementation and mathematical background of RCC can be found in [17, 20].

3. Simulation Study and Results

In order to validate the proposed concept, simulation was carried out using the power system toolbox of MATLAB / SIMULINK. The parameters used for the simulation are shown in Table 1. The simulation setup consists of three H-bridge inverters fed by a single PV panel of rating 60 W connected in series. The PV panel was modelled according to the parameters of commercial Solarex MSX-60 type using mathematical equations. A solar emulator may also be employed for emulating the characteristics of a real PV module [22]. The setup was tested for two different operating conditions; one with uniform irradiation where the panels are being subjected to the same level of irradiation resulting in identical DC link voltages and another is with nonuniform irradiation resulting in uneven DC link voltages.

3.1. Uniform irradiation condition

In order to verify the effectiveness of the proposed control scheme, the system is initially subjected to uniform irradiation. A change in the irradiation level from 1000 W/m^2 is applied at t = 1 s then after it decreases gradually till t = 1.1 s and is held constant at 600 W/m^2 till t = 1.3 s. From t = 1.3 s the irradiation level increases and settles back to 1000 W/m^2 at t = 1.4 s. This kind of irradiation profile is more practical since the variation in irradiation on any sunny day is similar to the chosen profile. The corresponding results are shown in Fig. 5. The upper plot, Fig. 5 (a) shows the change in PV current which is maintained at 3.5 A till t = 1 s ensuring the maximum power transfer from the panels.

Table 1. Various parameters of the proposed PV system

Parameter	Value	Unit
PV Panel (MSX-60)		
Short circuit current	3.8	A
Open circuit voltage	21.1	V
STC Voltage	17.1	V
STC Current	3.5	A
Power component ratings		
Grid voltage (RMS)	28	V
Grid frequency	50	Hz
Maximum grid current (RMS)	6.4	A
DC link capacitors	3.3	mF
Filter inductance	1.2	mH
Switching frequency	3	kHz
Controller values		
PR controller K_p K_r	 06 1000	
PI controller K_p K_I	 0.9 3	

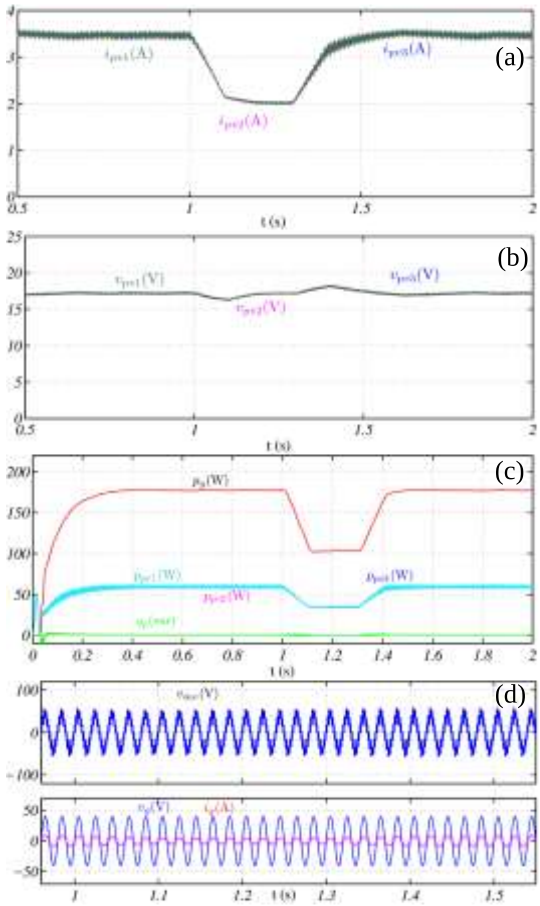

Fig. 5. Simulation results for the uniform change in irradiation

The RCC MPPT controller is able to track and maintain the operating point of all the PV panels around the MPP corresponding to its own irradiation level which is evident from plots of Fig. 5 (b),(c). The change in grid current and inverter voltage is shown in Fig. 5 (d).

3.2. Nonuniform irradiation condition

In the practical field, all the panels are not always subjected to the same level of irradiation. Hence the system was also tested for nonuniform level of irradiation wherein each panel was subjected to different irradiations shown in Table 2.

Table 2. Non uniform irradiation levels and their correspoding instants

	t = 1 s	t = 1.1 s	t = 1.3 s	t = 1.4 s
PV1	1000 W/m^2 to 600 W/m^2	600 W/m^2	600 W/m^2	600 W/m^2 to 1000 W/m^2
PV2	1000 W/m^2	1000 W/m^2	1000 W/m^2	1000 W/m^2
PV3	1000 W/m^2 to 800 W/m^2	800 W/m^2	800 W/m^2	800 W/m^2 to 1000 W/m^2

Simulation results are depicted various operating waveforms are shown in Fig. 6. From plot (a-b) of Fig. 6 it is evident that even with panels being subjected to different values of irradiation the MPPT controller is able to keep the individual operating points near MPP corresponding to its peculiar irradiation. Fig. 6(c) indicates the amount of active and reactive power being injected into the grid and also the power being extracted from each panel. Since the reactive current reference is set to zero reactive power injected to grid is almost maintained at zero with the operating power factor of unity. The change in temperature also affects the power generated by the PV system. To study this, PV panels were subjected to the temperature profile listed in Table 3.

The corresponding PV panels' current, voltage and power for change in temperature level is shown in Fig. 7.

Table 3. Non uniform temperature levels and their correspoding instants

	t = 1 s	t = 1.1 s
PV1	25^0C to 40^0C	40^0C to 25^0C
PV2	25^0C to 30^0C	30^0C to 45^0C
PV3	25^0C to 30^0C	30^0C

In addition to active power control it is expected from the distributed generation sources to perform ancillary functions like reactive power control, active power filtering, and bus voltage control. Hence the reactive power handling capability of the proposed system was tested by applying a step change in reference reactive power from zero to -100 Var at t = 0.5 s and from -100 Var to 100 Var at t = 0.6 s. Fig. 8 shows the waveforms corresponding to the step change in reactive power reference. From Fig. 8 (a) it can be seen that the system is able to inject/draw the commanded reactive power from/into the grid with maintaining the active power injected at its MPP.

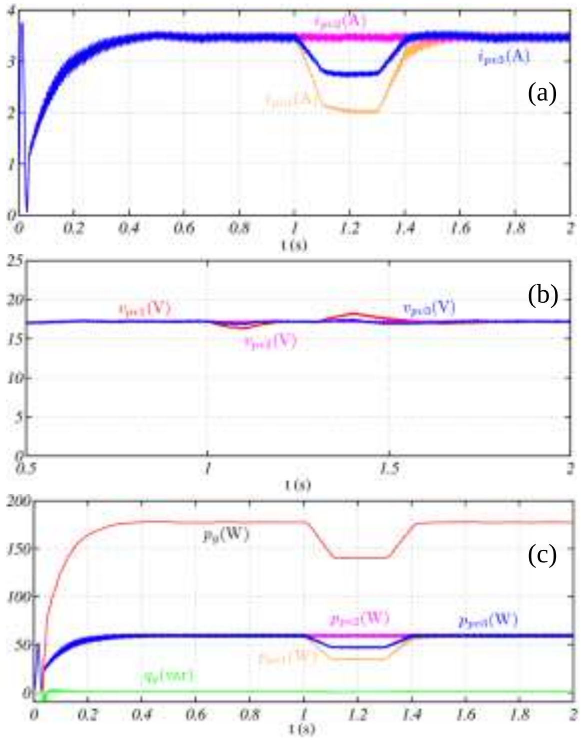

Fig. 6. Simulation results for the non uniform change in irradiation

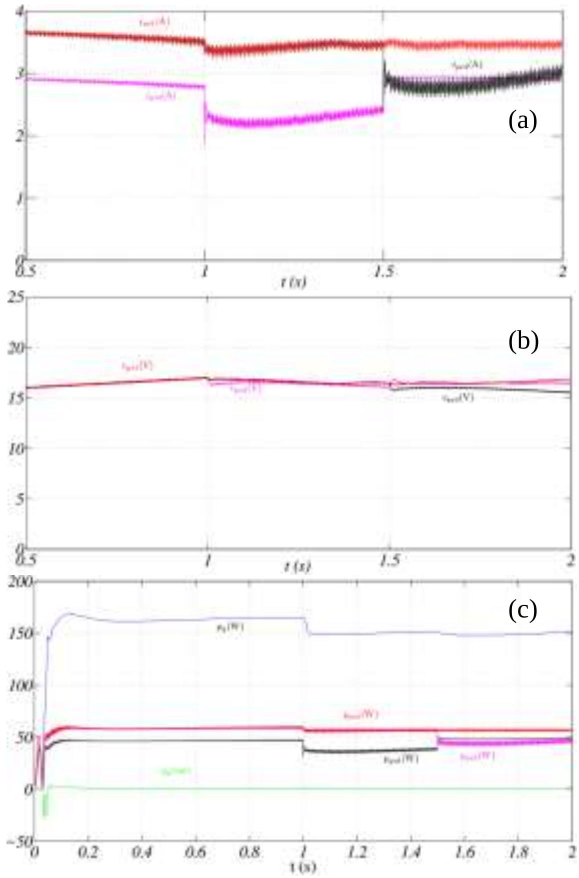

Fig. 7. Simulation results for the non uniform change in temperature

The corresponding phase shift in the grid current with respect to grid voltage is shown in Fig. 8 (b). Till t = 0.5 s the grid current is in phase with the voltage, after the step change in reference, the grid current leads the voltage thereby absorbing the reactive power till t = 0.6 s. Practically the grid voltage is not a pure sinusoidal wave and thus consists of a certain amount of harmonics which is also a cause for grid current distortion. Fig. 8 (c) demonstrates that the total harmonic distortion (%THD) in grid current is 2.91% in spite of harmonic present in the grid voltage thus complying the IEEE 519-1992 STD limits.

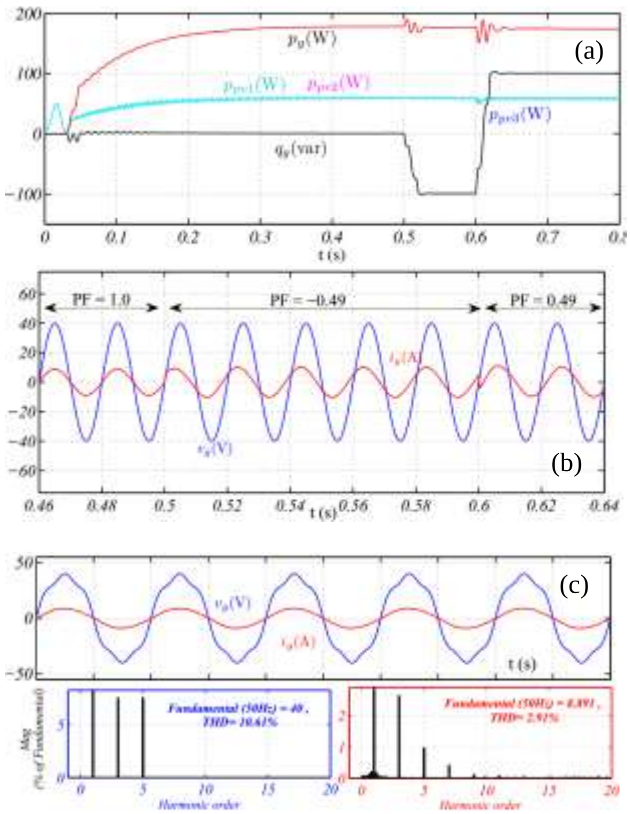

Fig. 8. Simulation results for step change in reactive power

4. Conclusion

This paper has proposed a control scheme for grid connected CHBMLI with PV generation. The advantage of the proposed system comes from the fact that it is able to generate high-quality currents, the capability to operate at a low switching frequency, and also its modular structure. RCC employed for MPPT is in a position to maintain the operating point each PV panel at its MPP for continuously changing irradiation levels. The control system embedded is in a position to injecting grid current with an arbitrary power factor keeping the maximum power injected into the grid intact. From the results, it is evident that the proposed control scheme can accurately track the MPP and also control the inverter such that the grid current with low harmonic distortion is injected turning it into a viable solution for grid connected string/multi-string technology.

References

[1] F. Blaabjerg, R. Teodorescu, M. Liserre and A. V. Timbus, "Overview of Control and Grid Synchronization for Distributed Power Generation Systems," IEEE Transactions on Industrial Electronics, vol. 53, no. 5, pp. 1398-1409, Oct. 2006.

[2] E. Romero-Cadaval, G. Spagnuolo, L. G. Franquelo, C. A. Ramos-Paja, T. Suntio and W. M. Xiao, "Grid-Connected Photovoltaic Generation Plants: Components and Operation," IEEE Industrial Electronics Magazine, vol. 7, no. 3, pp. 6-20, Sept. 2013.

[3] S. Daher, J. Schmid and F. L. M. Antunes, "Multilevel Inverter Topologies for Stand-Alone PV Systems," IEEE Transactions on Industrial Electronics, vol. 55, no. 7, pp. 2703-2712, July 2008.

[4] J. Rodriguez, Jih-Sheng Lai and Fang Zheng Peng, "Multilevel inverters: a survey of topologies, controls, and applications," in IEEE Transactions on Industrial Electronics, vol. 49, no. 4, pp. 724-738, Aug. 2002.

[5] M. Calais, V. G. Agelidis, M. Meinhardt, "Multilevel converters for single-phase grid connected photovoltaic systems: an overview", Solar Energy, vol. 66, no. 5, 325-335, Aug. 1999.

[6] V. Pires, J.F. Martins, D. Foito, H. Chen, "A grid connected photovoltaic system with a multilevel inverter and a Le-Blanc transformer", International Journal of Renewable Energy Research (IJRER), vol. 2, no. 1, 84-91, 2012.

[7] F. Richardeau and T. T. L. Pham, "Reliability Calculation of Multilevel Converters: Theory and Applications," IEEE Transactions on Industrial Electronics, vol. 60, no. 10, pp. 4225-4233, Oct 2013.

[8] R. Gonzalez, E. Gubia, J. Lopez and L. Marroyo, "Transformerless Single-Phase Multilevel-Based Photovoltaic Inverter," IEEE Transactions on Industrial Electronics, vol. 55, no. 7, pp. 2694-2702, July 2008.

[9] R. Selvamuthukumaran, A. Garg and R. Gupta, "Hybrid Multicarrier Modulation to Reduce Leakage Current in a Transformerless Cascaded Multilevel Inverter for Photovoltaic Systems," IEEE Transactions on Power Electronics, vol. 30, no. 4, pp. 1779-1783, Apr. 2015.

[10] O. Alonso, P. Sanchis, E. Gubia and L. Marroyo, "Cascaded H-bridge multilevel converter for grid connected photovoltaic generators with independent maximum power point tracking of each solar array,"Power Electronics Specialist Conference, 2003. PESC '03. 2003 IEEE 34th Annual, 2003, pp. 731-735 vol.2.

[11] E. Villanueva, P. Correa, J. Rodriguez and M. Pacas, "Control of a Single-Phase Cascaded H-Bridge Multilevel Inverter for Grid-Connected Photovoltaic Systems," IEEE Transactions on Industrial Electronics, vol. 56, no. 11, pp. 4399-4406, Nov. 2009.

[12] B. R. Lin and H. H. Lu, "New multilevel rectifier based on series connection of H-bridge cell," IEE Proceedings - Electric Power Applications, vol. 147, no. 4, pp. 304-312, Jul 2000.

[13] C. Cecati, A. Dell'Aquila, M. Liserre and V. G. Monopoli, "A passivity-based multilevel active rectifier

with adaptive compensation for traction applications," IEEE Transactions on Industry Applications, vol. 39, no. 5, pp. 1404-1413, Sept.-Oct. 2003.

[14] M. A. G. de Brito, L. Galotto, L. P. Sampaio, G. d. A. e Melo and C. A. Canesin, "Evaluation of the Main MPPT Techniques for Photovoltaic Applications," IEEE Transactions on Industrial Electronics, vol. 60, no. 3, pp. 1156-1167, March 2013.

[15] B. Subudhi and R. Pradhan, "A Comparative Study on Maximum Power Point Tracking Techniques for Photovoltaic Power Systems," IEEE Transactions on Sustainable Energy, vol. 4, no. 1, pp. 89-98, Jan. 2013.

[16] S. Jain and V. Agarwal, "Comparison of the performance of maximum power point tracking schemes applied to single-stage grid-connected photovoltaic systems," IET Electric Power Applications, vol. 1, no. 5, pp. 753-762, Sept. 2007.

[17] T. Esram and P. L. Chapman, "Comparison of Photovoltaic Array Maximum Power Point Tracking Techniques," IEEE Transactions on Energy Conversion, vol. 22, no. 2, pp. 439-449, June 2007.

[18] D. Casadei, G. Grandi and C. Rossi, "Single-phase single-stage photovoltaic generation system based on a ripple correlation control maximum power point tracking," IEEE Transactions on Energy Conversion, vol. 21, no. 2, pp. 562-568, June 2006.

[19] Sandeep. N and Udaykumar R Y, "Single-phase modular multilevel inverter based grid-connected photovoltaic system," 2015 Annual IEEE India Conference (INDICON), New Delhi, 2015, pp. 1-6.

[20] T. Esram, J. W. Kimball, P. T. Krein, P. L. Chapman and P. Midya, "Dynamic Maximum Power Point Tracking of Photovoltaic Arrays Using Ripple Correlation Control," IEEE Transactions on Power Electronics, vol. 21, no. 5, pp. 1282-1291, Sept. 2006.

[21] Sandeep. N, Mutta Krishna Murthy and P. S. Kulkarni, "Single-phase grid-connected photovoltaic system based on ripple correlation control maximum power point tracking," Electrical, Electronics and Computer Science (SCEECS), 2014 IEEE Students' Conference on, Bhopal, 2014, pp. 1-6.

[22] Balakishan. C and Sandeep. N, "Development of a microcontroller based PV emulator with current controlled DC/DC buck converter," International Journal of Renewable Energy Research (IJRER), vol. 4, no. 4, 1049-1055, 2014.